iScience, Volume *25*

Supplemental information

The role of bivalent ions in the regulation of D-loop extension mediated by DMC1 during meiotic recombination

Veronika Altmannova, Mario Spirek, Lucija Orlic, Atis Jēkabsons, Tereza Clarence, Adrian Henggeler, Jarmila Mlcouskova, Raphaël A.G. Chaleil, Joao Matos, and Lumir Krejci

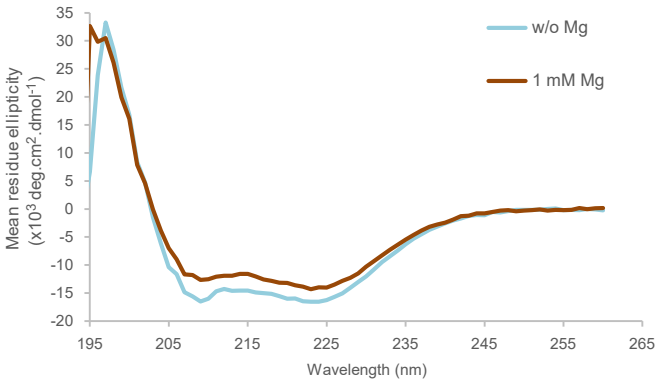

Figure S1, related to Figure 1A. *Effect of magnesium ions on the secondary structure of DMC1.* CD spectra of the human DMC1 protein (5 µM) in the presence of ATP (0.3 mM) and in the absence (light blue line) or in the presence of 1 mM $MgCl_2$ (brown line).

A

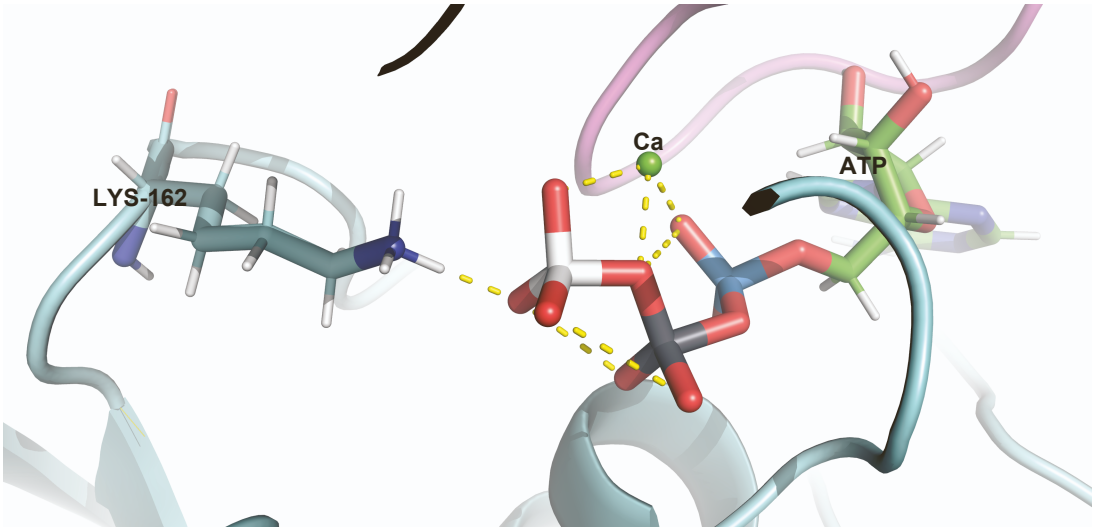

B

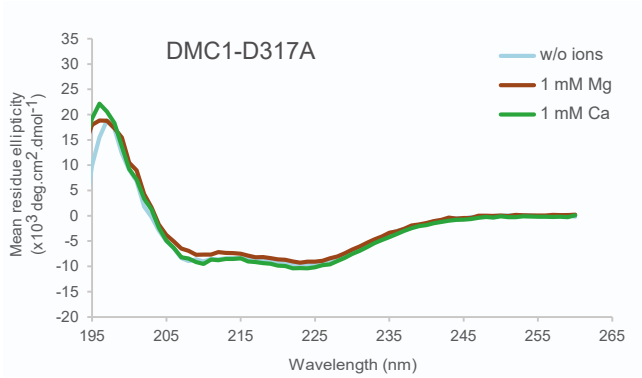

C

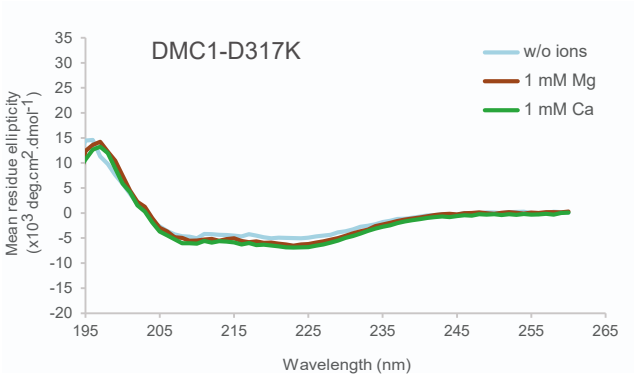

D

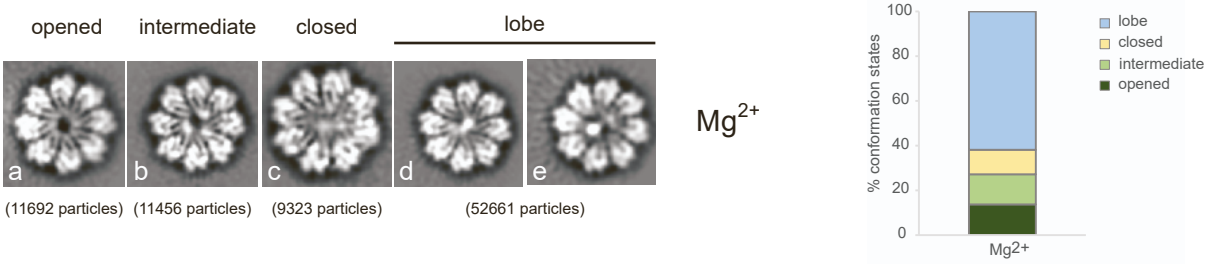

Image	Conformation state	RGB scale	Outer particle diameter, Å	Inner particle diameter, Å
a	opened	0	131	16
b	intermediate	41	135	12
c	closed	176	137	n.a.
d	lobe	255	138	n.a.
e	lobe	255	138	n.a.

Figure S2, related to Figure 2. *Structural and biophysical analysis of DMC1 mutants.* (A) Molecular simulation of DMC1-E162K in the presence of Ca^{2+} and ATP. (B) CD spectra of the human DMC1-D317A mutant (5 μM) and ATP (0.3 mM), in the absence of bivalent ions (light blue line) or in the presence of 1 mM $MgCl_2$ (brown line) or 1 mM $CaCl_2$ (green line), respectively. (C) CD spectra of the human DMC1-D317K mutant (5 μM) and ATP (0.3 mM), in the absence of bivalent ions (light blue line) or in the presence of 1 mM $MgCl_2$ (brown line) or 1 mM $CaCl_2$ (green line), respectively. (D) 2D class averages of cryo-EM particles of human DMC1-D317K mutant in the presence of $MgCl_2$ and ATP representing "opened" (a), "intermediate" (b), "closed" (c) and "lobe" (d and e) states. Classification of individual states was based on RGB scale in range from 0 (black color) to 255 (white color), respectively. The intensity in RGB scale 1-50 corresponds to opened, 51-100 to intermediate, 101-200 to closed, and 201-300 to lobe forms, respectively.

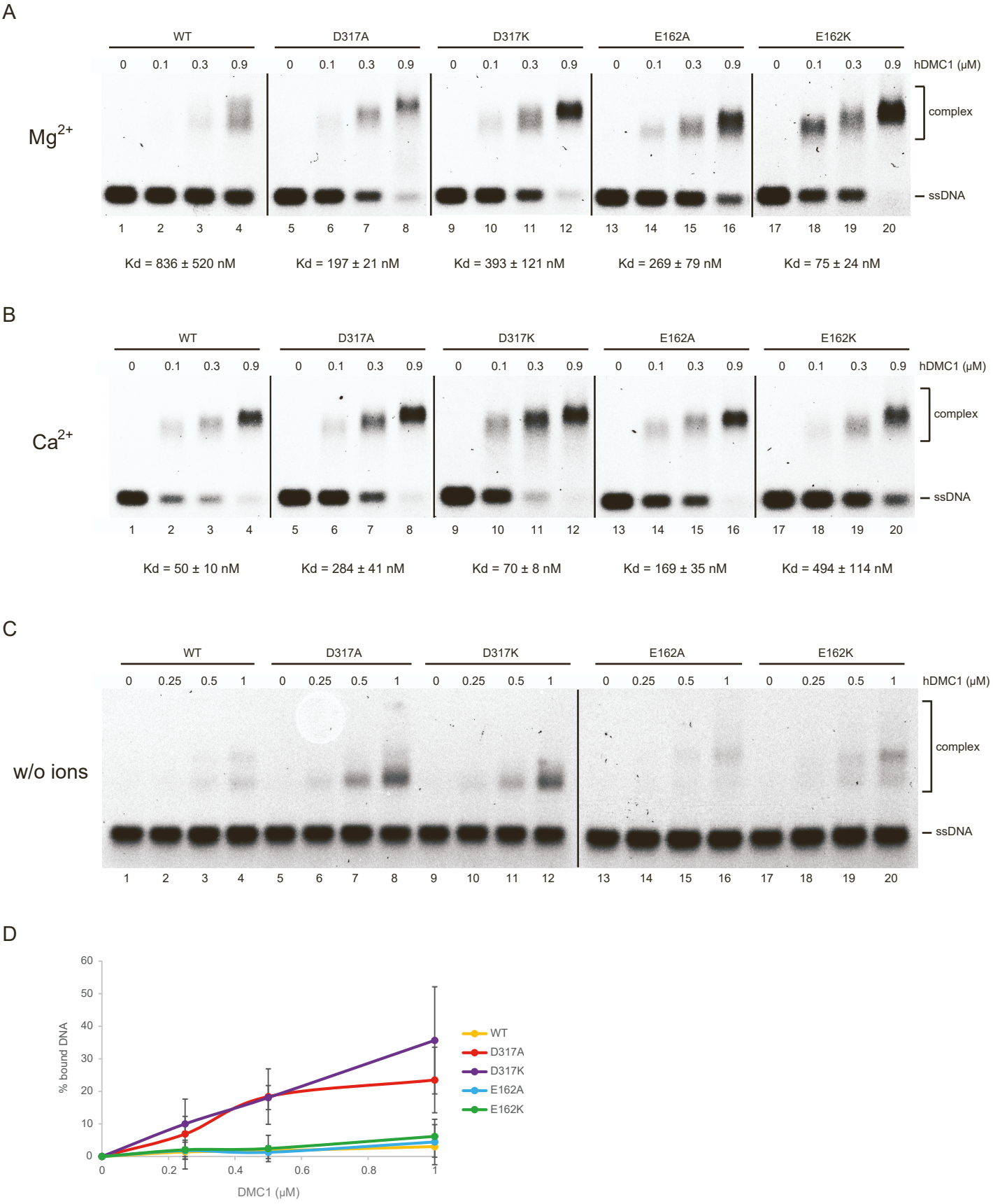

Figure S3, related to Figure 2. *ssDNA binding activity of DMC1 mutants.* (A) Representative gels of data from Figure 2D including the dissociation constants of DNA binding affinity. The Kd values were calculated using GraphPad Prism software. (B) Representative gels of data from Figure 2E including the dissociation constants of DNA binding affinity. The Kd values were calculated using GraphPad Prism software. (C) DNA binding of DMC1 mutants (0.25, 0.5 and 1 μM) to 5'-fluorescently labeled ssDNA (pR231, 0.9 μM nucleotides) in the absence of bivalent ions analyzed by gel-based assay. (D) Graphical representation of data from (C). The error bars represent the standard deviation from three independent experiments.

A

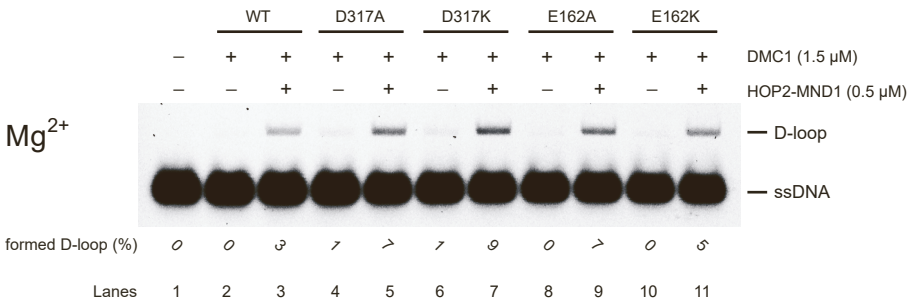

B

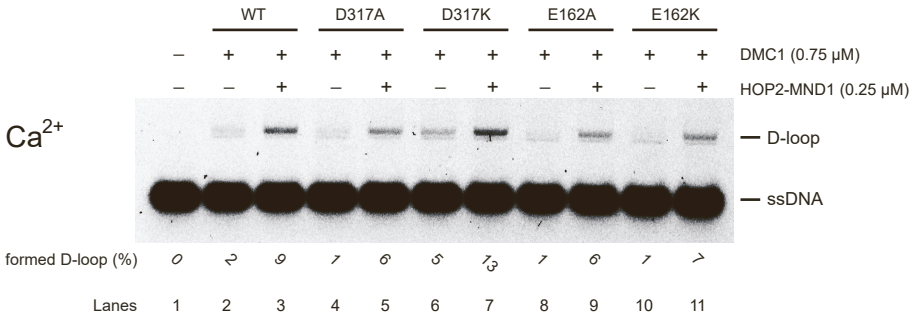

Figure S4, related to Figure 3. *HOP2-MND1 stimulates D-loop activity of DMC1 mutants.* (A) DMC1 mutants (1.5 μM) were incubated with fluorescently labeled 90-mer ssDNA in the presence of 1 mM $MgCl_2$. HOP2-MND1 complex (0.5 μM) was added to the indicated reactions followed by the addition of pBluescript plasmid DNA. (B) DMC1 mutants (0.75 μM) were incubated with fluorescently labeled 90-mer ssDNA in the presence of 1 mM $CaCl_2$. HOP2-MND1 complex (0.25 μM) was added to the indicated reactions followed by the addition of pBluescript plasmid DNA.

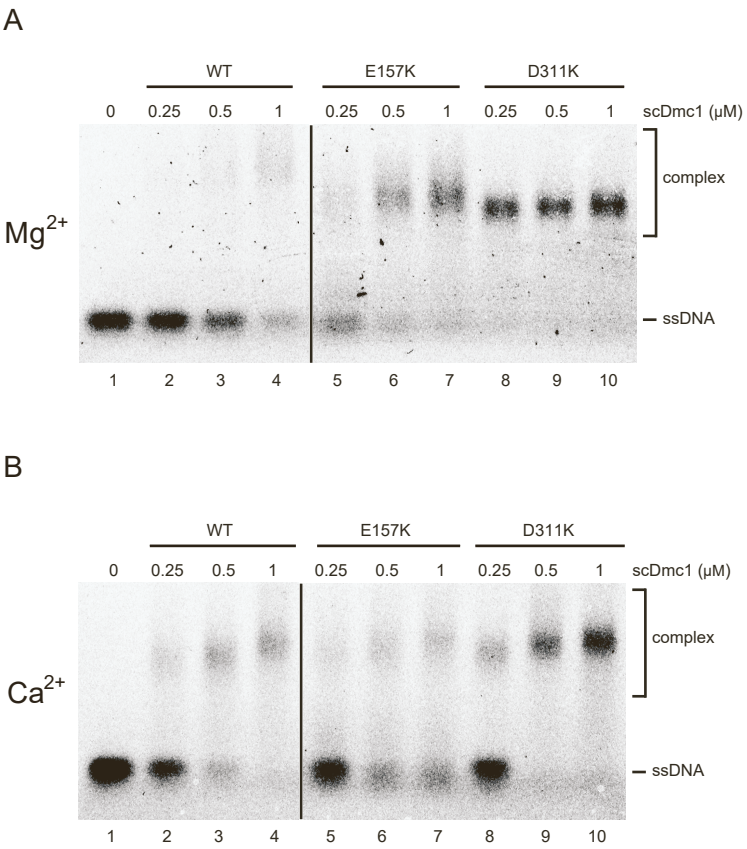

Figure S5, related to Figure 5. *ssDNA binding activity of yeast Dmc1 mutants.* (A) Representative gels of data from Figure 5B. (B) Representative gels of data from Figure 5C.

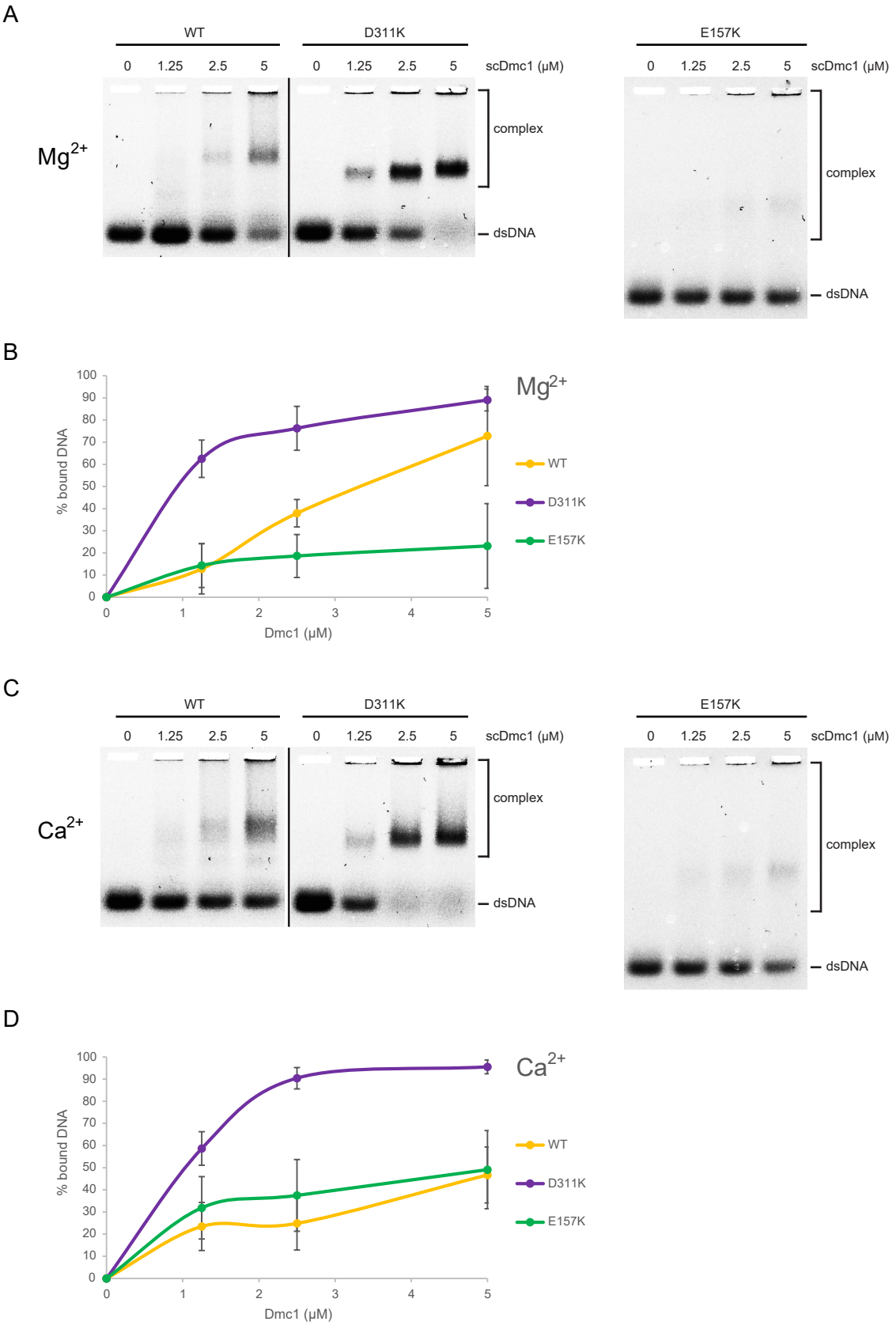

Figure S6, related to Figure 5. *dsDNA binding activity of yeast Dmc1 mutants.* (A) DNA binding of Dmc1 mutants (1.25, 2.5 and 5 μM) to 5'-fluorescently labeled dsDNA (0.5 μM base pairs) in the presence of 1 mM ATP and 1 mM $MgCl_2$ analyzed by gel-based assay. (B) Graphical representation of data from (A). The error bars represent the standard deviation from three independent experiments. (C) DNA binding of Dmc1 mutants (1.25, 2.5 and 5 μM) to 5'-fluorescently labeled dsDNA (0.5 μM base pairs) in the presence of 1 mM ATP and 1 mM $CaCl_2$ analyzed by gel-based assay. (D) Graphical representation of data from (C). The error bars represent the standard deviation from three independent experiments.

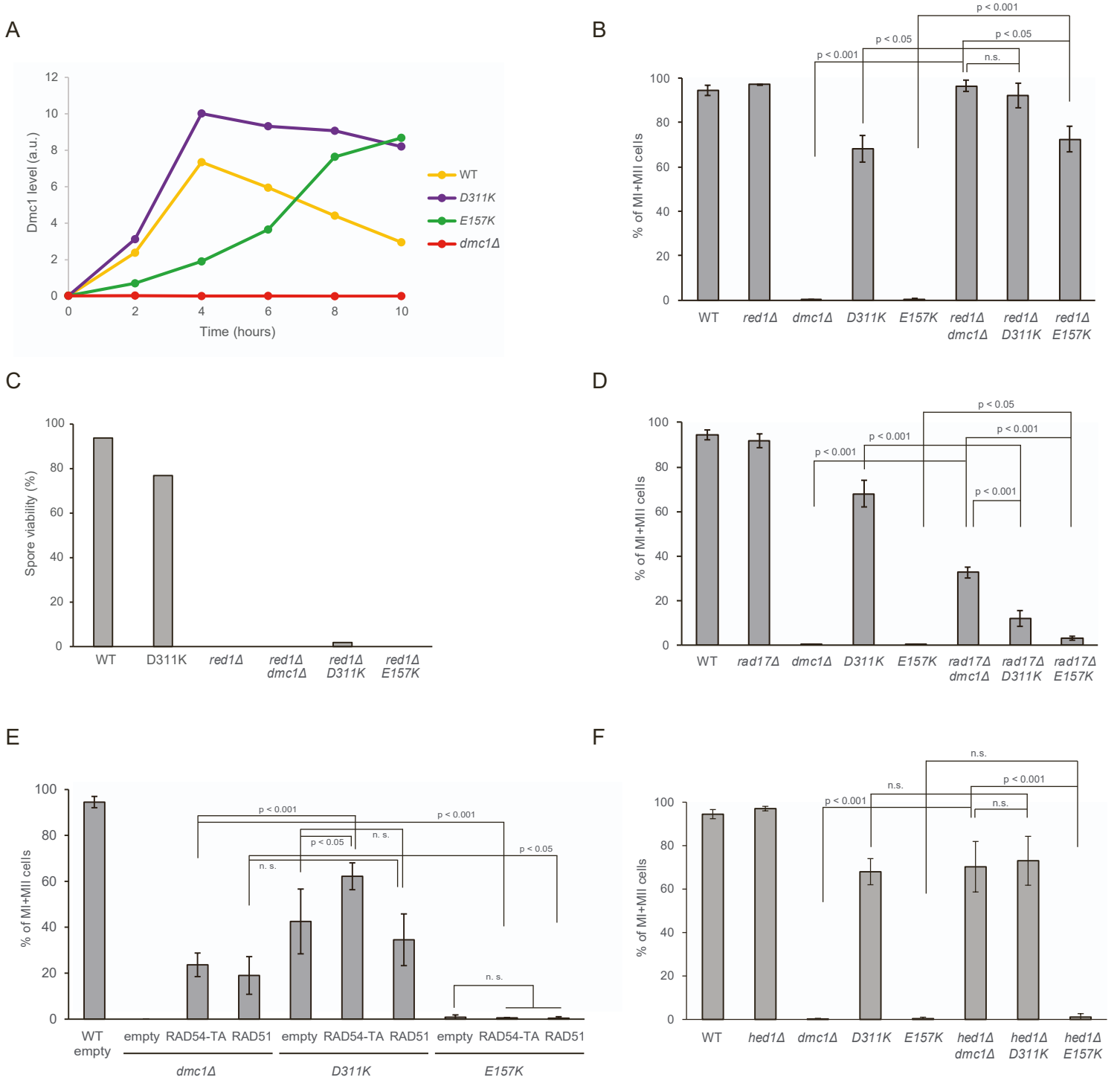

Figure S7, related to Figure 5. *Phenotypic characterization of yeast dmc1 mutants.* (A) The quantification of Dmc1 signal from Figure 5D. The signal was corrected to amount of loading control of PGK1 signal, and subsequently normalized to signal of unspecific band at 6 hours. (B) DAPI analysis of meiotic divisions in *dmc1* mutants in *red1* deletion background. The analysis was done as in Figure 5E. (C) Spore viability of selected *dmc1* strains. Spore viability was assayed by tetrad dissection of 40 diploid colonies for each strain. (D) DAPI analysis of meiotic divisions in *dmc1* mutants in *rad17* deletion background. The analysis was done as in Figure 5E. (E) DAPI analysis of meiotic divisions in *dmc1* mutants in strains overexpressing Rad51 or Rad54-T132A mutant, respectively. Cells were harvested after 12 hours after synchronous induction of meiosis and the analysis was done as in Figure 5E except of for wt at least 65 cells were analyzed from each culture. (F) DAPI analysis of meiotic divisions in *dmc1* mutants in *hed1* deletion background. The analysis was done as in Figure 5E.

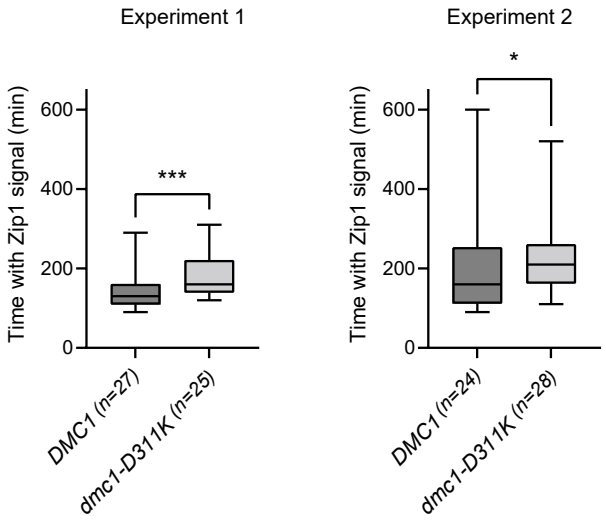

Figure S8, related to Figure 6. *Duration of Zip1 signal in dmc1 strains.* Box plot depicts median with lower and upper quartile of the duration of *dmc1Δ/DMC1* and *dmc1Δ/dmc1-D311K* cells having accumulated Zip1 signal. Whiskers represent minimum and maximum (two-tailed unpaired t test; *p < 0.05, **p < 0.01). The two independent experiments are shown separately.

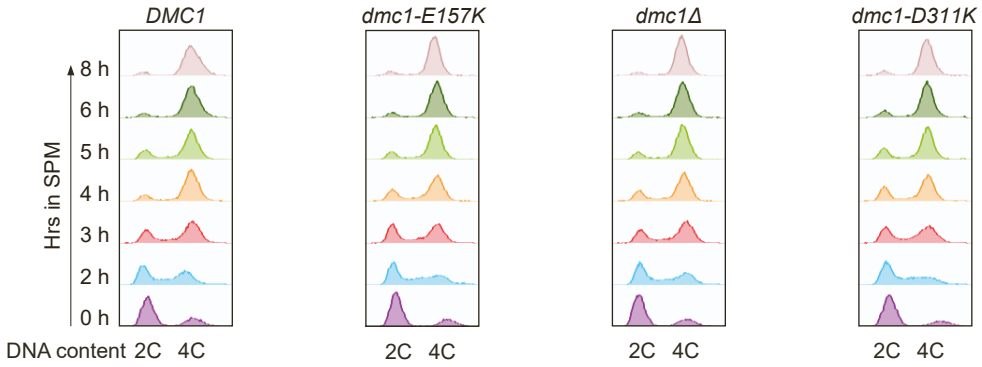

Figure S9, related to Figure 7. *FACS analysis of meiotic progression of dmc1 strains. S. cerevisiae* strains with the indicated genotypes were synchronously released to undergo meiosis from G0/G1 by transferring cells into sporulation medium (SPM). Cells were collected at indicated time points and DNA content was analyzed by fluorescence-activated cell-sorting. The image shown is representative of two independent experiments.

Table S1 (related to STAR Methods). Oligonucleotides used in the study.

Name	Sequence
hDMC1-D317A fwd	TTGCCAAGATTTATGCCAGTCCTGAGATGCC
hDMC1-D317A rev	GGCATCTCAGGACTGGCATAAATCTTGGCAA
hDMC1-D317K fwd	GGAGAGCTCAGAATTGCCAAGATTTATAAGAGTCCTGAGATGCC
hDMC1-D317K rev	GGCATCTCAGGACTCTTATAAATCTTGGCAATTCTGAGCTCTCC
hDMC1-E162A fwd	TCTTCATTGATACAGCAAATACTTTCCGTCC
hDMC1-E162A rev	GGACGGAAAGTATTTGCTGTATCAATGAAGA
hDMC1-E162K fwd	GCGATCTGGACGGAAAGTATTTTTTGTATCAATGAAGATAATCTTTC
hDMC1-E162K rev	GAAAGATTATCTTCATTGATACAAAAAATACTTTCCGTCCAGATCGC
scDmc1-D311K fwd	AGTTGCCAAGTTACAAAAATCCCCAGATATGCCTG
scDmc1-D311K rev	CAGGCATATCTGGGGATTTTTGTAACTTGGCAACT
scDmc1-E157K fwd	CGGGCCTGAAAGTGCCTTTTGTATCAATATATGCTACTTTC
scDmc1-E157K rev	GAAAGTAGCATATATTGATACAAAAGGCACTTTCAGGCCCG
pR231	AAATCAATCTAAAGTATATATGAGTAAACTTGGTCTGACAGTTACCAATGCTTAATC AGTGAGGCACCTATCTCAGCGATCTGTCTATTT
pR27	AGCTACCATGCCTGCACGAATTAAGCAATTCGTAATCATGGTCATAGCT
pR28	AGCTATGACCATGATTACGAATTGCTTAATTCGTGCAGGCATGGTAGCT
Δred1 fwd	GAACAAAGATTTTTTAATCAGTGAGGACCACAAAGGGACAGCAAATACGGTGATAAG ACGTACGCTGCAGGTCGAC
Δred1 rev	CTTTTATTAGCCATCTTAAATCTAAAAAGAATTGCGTATATGTATACTATTTAATCG ATGAATTCGAGCTCG
Δrad17 fwd	CAAATCAATCTCACAGAACGGTGTGGAAACAAAGTAGTTGAAGGATTTCAACTCGTA CGCTGCAGGTCGAC
Δrad17 rev	CCAAATGCTGAATGAAGTTCTGCGTTTTCTGCGATGCTGGATATTGACTTAATCGAT GAATTCGAGCTCG
Δhed1 fwd	GGTTAAATTCTTGAATTACAACTACATGTCAGAGACGAACGAAAGAGAGAAATCAAG ACGCGTACGCTGCAGGTCGAC
Δhed1 rev	ACGTTGAAAAAAGTGGAGGGCCACCGAACTCTTTTTCAAACGTTCTCCTCTTTGAAC TTAATCGATGAATTCGAGCTCG

Table S2 (related to STAR Methods). Yeast strains used in this study.

Strain	Genotype	Source
NHY1210	MATa ho::hisG leu2::hisG ura3(ΔSma-Pst) HIS4::LEU2-(BamHI; +ori)	N. Hunter
NHY1215	MATα ho::hisG leu2::hisG ura3(ΔSma-Pst) his4-X::LEU2-(NgoMIV; +ori)	N. Hunter
yLK561	MATa ho::hisG leu2::hisG ura3(ΔSma-Pst) HIS4::LEU2-(BamHI; +ori) dmc1-D311K	This study
yLK562	MATα ho::hisG leu2::hisG ura3(ΔSma-Pst) his4-X::LEU2-(NgoMIV; +ori) dmc1-D311K	This study
yLK565	MATa ho::hisG leu2::hisG ura3(ΔSma-Pst) HIS4::LEU2-(BamHI; +ori) dmc1-E157K	This study
yLK566	MATα ho::hisG leu2::hisG ura3(ΔSma-Pst) his4-X::LEU2-(NgoMIV; +ori) dmc1-E157K	This study
yLK575	MATa ho::hisG leu2::hisG ura3(ΔSma-Pst) HIS4::LEU2-(BamHI; +ori) Δdmc1::kanMX4	This study
yLK578	MATα ho::hisG leu2::hisG ura3(ΔSma-Pst) his4-X::LEU2-(NgoMIV; +ori) Δdmc1::kanMX4	This study
yLK540	MATa ho::hisG leu2::hisG ura3(ΔSma-Pst) HIS4::LEU2-(BamHI; +ori) dmc1-D311K Δred1::natMX	This study
yLK541	MATα ho::hisG leu2::hisG ura3(ΔSma-Pst) his4-X::LEU2-(NgoMIV; +ori) dmc1-D311K Δred1::natMX	This study
yLK545	MATa ho::hisG leu2::hisG ura3(ΔSma-Pst) HIS4::LEU2-(BamHI; +ori) dmc1-E157K Δred1::natMX	This study
yLK550	MATα ho::hisG leu2::hisG ura3(ΔSma-Pst) his4-X::LEU2-(NgoMIV; +ori) dmc1-E157K Δred1::natMX	This study
yLK514	MATa ho::hisG leu2::hisG ura3(ΔSma-Pst) HIS4::LEU2-(BamHI; +ori) Δred1::natMX	This study
yLK527	MATα ho::hisG leu2::hisG ura3(ΔSma-Pst) his4-X::LEU2-(NgoMIV; +ori) Δred1::natMX	This study
yLK557	MATa ho::hisG leu2::hisG ura3(ΔSma-Pst) HIS4::LEU2-(BamHI; +ori) Δdmc1::kanMX4 Δred1::natMX	This study
yLK558	MATα ho::hisG leu2::hisG ura3(ΔSma-Pst) his4-X::LEU2-(NgoMIV; +ori) Δdmc1::kanMX4 Δred1::natMX	This study
yLK581	MATa ho::hisG leu2::hisG ura3(ΔSma-Pst) HIS4::LEU2-(BamHI; +ori) dmc1-D311K Δrad17::natMX	This study
yLK580	MATα ho::hisG leu2::hisG ura3(ΔSma-Pst) his4-X::LEU2-(NgoMIV; +ori) dmc1-D311K Δrad17::natMX	This study
yLK582	MATa ho::hisG leu2::hisG ura3(ΔSma-Pst) HIS4::LEU2-(BamHI; +ori) dmc1-E157K Δrad17::natMX	This study
yLK579	MATα ho::hisG leu2::hisG ura3(ΔSma-Pst) his4-X::LEU2-(NgoMIV; +ori) dmc1-E157K Δrad17::natMX	This study
yLK506	MATa ho::hisG leu2::hisG ura3(ΔSma-Pst) HIS4::LEU2-(BamHI; +ori) Δrad17::natMX	This study
yLK507	MATα ho::hisG leu2::hisG ura3(ΔSma-Pst) his4-X::LEU2-(NgoMIV; +ori) Δrad17::natMX	This study
yLK483	MATa ho::hisG leu2::hisG ura3(ΔSma-Pst) HIS4::LEU2-(BamHI; +ori) Δdmc1::kanMX4 Δrad17::natMX	This study
yLK543	MATα ho::hisG leu2::hisG ura3(ΔSma-Pst) his4-X::LEU2-(NgoMIV; +ori) Δdmc1::kanMX4 Δrad17::natMX	This study
yLK433	MATa ho::hisG leu2::hisG ura3(ΔSma-Pst) HIS4::LEU2-(BamHI; +ori) Δhed1::natMX	This study
yLK440	MATα ho::hisG leu2::hisG ura3(ΔSma-Pst) his4-X::LEU2-(NgoMIV; +ori) Δhed1::natMX	This study
yLK436	MATa ho::hisG leu2::hisG ura3(ΔSma-Pst) HIS4::LEU2-(BamHI; +ori) Δdmc1::kanMX4 Δhed1::natMX	This study
yLK437	MATα ho::hisG leu2::hisG ura3(ΔSma-Pst) his4-X::LEU2-(NgoMIV; +ori) Δdmc1::kanMX4 Δhed1::natMX	This study

yLK449	MATa ho::hisG leu2::hisG ura3(ΔSma-Pst) HIS4::LEU2-(BamHI; +ori) Δhed1::natMX dmc1-D311K	This study
yLK443	MATα ho::hisG leu2::hisG ura3(ΔSma-Pst) his4-X::LEU2-(NgoMIV; +ori) Δhed1::natMX dmc1-D311K	This study
yLK434	MATa ho::hisG leu2::hisG ura3(ΔSma-Pst) HIS4::LEU2-(BamHI; +ori) Δhed1::natMX dmc1-E157K	This study
yLK435	MATα ho::hisG leu2::hisG ura3(ΔSma-Pst) his4-X::LEU2-(NgoMIV; +ori) Δhed1::natMX dmc1-E157K	This study
YJM13677	*MATa/MATalpha dmc1Δ::KanMX4/DMC1 ZIP1::GFP(700)-HphMX4/ZIP1 CNM67-tdTomato-NatMX4/ CNM67 his4-X::LEU2-(NgoMIV; +ori)/HIS4::LEU2*	This study
YJM13678	*MATa/MATalpha dmc1Δ::KanMX4/dmc1-D311K ZIP1::GFP(700)-HphMX4/ZIP1 CNM67-tdTomato-NatMX4/ CNM67 his4-X::LEU2-(NgoMIV; +ori)/HIS4::LEU2*	This study
YJM13679	*MATa/MATalpha dmc1Δ::KanMX4/dmc1-E157K ZIP1::GFP(700)-HphMX4/ZIP1 CNM67-tdTomato-NatMX4/ CNM67*	This study
YJM13680	*MATa/MATalpha dmc1Δ::KanMX4 ZIP1::GFP(700)-HphMX4/ZIP1 CNM67-tdTomato-NatMX4/ CNM67*	This study
YJM13718	*MATa/MATalpha dmc1Δ::KanMX4/DMC1 ZIP1::GFP(700)-HphMX4/ZIP1 CNM67-tdTomato-NatMX4/ CNM67 his4-X::LEU2-(NgoMIV; +ori)/ HIS4::LEU2*	This study
YJM13719	*MATa/MATalpha dmc1Δ::KanMX4/dmc1-D311K ZIP1::GFP(700)-HphMX4/ZIP1 CNM67-tdTomato-NatMX4/ CNM67*	This study
YJM13720	*MATa/MATalpha dmc1Δ::KanMX4/dmc1-E157K ZIP1::GFP(700)-HphMX4/ZIP1 CNM67-tdTomato-NatMX4/ CNM67*	This study
YJM13721	*MATa/MATalpha dmc1Δ::KanMX4 ZIP1::GFP(700)-HphMX4/ZIP1 CNM67-tdTomato-NatMX4/ CNM67*	This study